CHEMISTRY OF MATERIALS

Article

pubs.acs.org/cm

Restructuring of Graphene Oxide Sheets into Monodisperse Nanospheres

Christopher D. Zangmeister,*[,†] Xiaofei Ma,[†,‡] and Michael R. Zachariah[†,‡]

[†]Material Measurement Laboratory, National Institute of Standards and Technology, Gaithersburg, Maryland, 20899, United States

[‡]Department of Mechanical Engineering and Department of Chemistry and Biochemistry, University of Maryland, College Park, Maryland 20742, United States .

Supporting Information

ABSTRACT: We demonstrate a method to restructure graphene oxide sheets into monodisperse solid 17 nm nanospheres by tuning the solution ionic strength. This method enables the preparation of both two-dimensional self-assemblies comprising three-dimensional GO nanospheres and three-dimensional super assemblies of GO clusters via dispersal into an aerosol. The GO super assemblies are more thermally stable than single crumpled sheets. Finally, we demonstrate that GO nanospheres and their assemblies can be thermally processed to form reduced GO with high aromatic character while still maintaining their spherical conformation.

KEYWORDS: *graphene, graphene oxide, aerosol, super assembly*

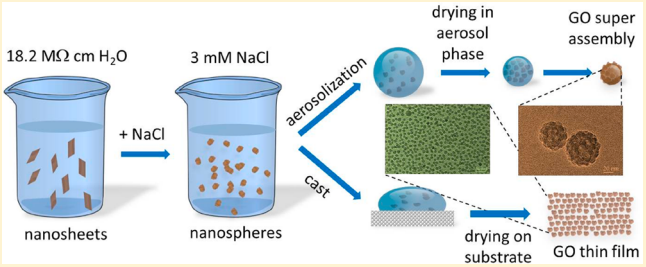

INTRODUCTION

Influencing the morphology in simple nanomaterials requires understanding and balancing steric effects, electrostatic forces, among other interactions, and has proven to be very challenging. In this study, we focus on controlling the nanoscale morphology of graphene oxide (GO), a flexible membrane-like material comprised of aromatic and oxygen functionalities that is also frequently used as a solution processable precursor to graphene.[1−9] In aqueous solution, GO exists as a planar sheet that can be cast onto solid surfaces to form large-scale two-dimensional arrays and subsequently thermally or chemically reduced to a conducting graphene-like (reduced GO or rGO) material. Although graphene and rGO properties have potential organic electronic[10] and charge carrier applications,[11,12] the intra- and intersheet aggregation behavior of both materials has made processing interfaces in and beyond two-dimensions difficult.[1] Three-dimensional graphene-based materials can be envisioned to have unique physical and chemical properties for new nanostructures[13] and nanofluids.[14]

Recent work in our laboratory showed that when GO nanosheets are aerosolized from aqueous solution they crumple by capillary forces upon rapid H_2O removal into self-avoiding sheets that are identical in conformation and fractal dimension to what is observed in macroscopic crumpled paper.[15]

In this investigation, we extend nanosheet crumpling into the solution phase by tuning the solution ionic strength. The effect of solution ionic strength are assessed by measuring the size distribution of GO as a function of solution ionic strength using dynamic light scattering and electronic (transmission and scanning) microscopies in samples prepared from solution and after aerosolization.

EXPERIMENTAL SECTION

GO Synthesis and Sample Preparation. GO was prepared using a modified version of the Hummer's synthetic scheme as described previously.[16] Dried GO powder was added to water at 0.5 mg/mL. The GO concentration was obtained by measuring the UV−vis absorption at 400 nm (5.75 mg mL^{-1} cm^{-1}). NaCl was added to a stock GO solution. From aerosol size distribution measurements, the transition from GO sheets to GO nanospheres occurs faster than the time scale of NaCl addition to completion of the measurement (<5 min). Thermal reduction of GO films was made in a temperature calibrated tube furnace in air (22% O_2). The aerosol residence time was 5 s using a 1.5 L min^{-1} flow rate. Thin films samples were drop cast onto solid surfaces and dried in a vacuum desiccator.

Dynamic Light Scattering (DLS). Light scattering measurements were made using a commercial DLS instrument. Due to sample absorption, samples were diluted 10:1, keeping the ionic strength constant for each DLS measurement.

Transmission Electron Microscopy (TEM). TEM measurements were made on a commercial instrument from GO films drop cast onto copper/SiO_2 grids. Images in solutions were acquired under cryogenic conditions (approximately −186 °C) using a 100 keV accelerating voltage. Typical operating conditions for other imaging conditions were at 200 keV acceleration voltage.

Aerosol Size Distribution. GO aerosol was formed by a commercial aerosol generator. The aerosol was quickly dried using two diffusion driers in series. The size distribution was made by first passing the aerosol through a diffusion mobility analyzer (DMA) with a 5 L/min sheath flow, and particles were then counted as a function

Received: April 10, 2012
Revised: June 5, 2012
Published: June 7, 2012

of particle size using a commercial condensation particle counter (CPC).

Aerosol Particle Mass Analyzer (APM). APM measurements were made as described in our previous work.[17−20] DMA conditions were identical to those used in the aerosol size distribution measurements.

X-ray Photoemission Spectroscopy (XPS). XPS measurements were made on a commercial multichannel X-ray photoemission spectrometer using a monochromatic Al kα source and 40 eV pass energy from samples cast onto cleaned metal surfaces.

RESULTS AND DISCUSSION

Size distributions measured by dynamic light scattering of aqueous GO (0.5 mg/mL), shown as black circles in Figure 1a, indicate that the hydrodynamic diameter of GO sheets in H_2O are distributed from about 400 nm to over 800 nm in size. Upon addition of NaCl (0.3 mmol/L), however, the particle size is shifted to a narrow distribution with a hydrodynamic diameter centered around 95 nm (red squares in Figure 1a). Cryo-TEM images obtained from the same solution in the free frozen state (−186 °C) confirm the absence of nanosheets and restructuring of GO to form nanospheres in aqueous NaCl solution, see inset of Figure 1a. TEM and SEM images are shown in Figure 1b for films dropcast from 18.2 MΩ cm H_2O and 3 mmol/L NaCl solutions. Aqueous GO sheets dropcast from 18.2 MΩ cm H_2O extend across the drop cast surface to form a smooth, 2-dimensional planar film, consisting of multiple overlying sheets. When GO is cast from a 3 mmol/L NaCl solution, it forms nanospheres or ovoids with an average diameter of 17.4 nm ±2.2 nm (1σ). The SEM image in Figure 1b illustrates that GO nanospheres cast from 3 mmol/L NaCl onto a surface form ordered, layered, self-assembled films over several square centimeters. Similar to the thin films and papers constructed from planar GO in our laboratory, multilayered films comprised of GO nanospheres were mechanically rigid, and were able to be peeled from a surface and handled without noticeable loss of physical integrity over macroscopic length scales.

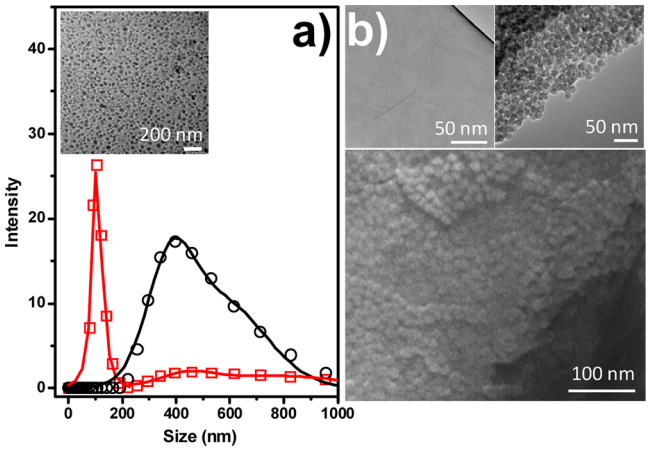

Figure 1. Dependence of ionic strength on aqueous graphene oxide solution. (a) Dynamic light scattering of aqueous 0.5 mg/mL GO solution in 18.2 MΩ cm H_2O (black circles) and 3.0 mmol/L NaCl (red squares). Inset shows TEM image obtained from GO in aqueous 0.3 mmol/L NaCl acquired at −186 °C in the free frozen state. (b) Clockwise from top left: TEM image of drop cast from 0.5 mg/mL GO in 18.2 MΩ cm H_2O, TEM image of film at film step interface from 3 mmol/L NaCl. Nanospheres are ∼17 nm, SEM image of dropcast GO film cast from 3 mM NaCl.

GO nanospheres are formed across a wide GO and NaCl concentration range. TEM images revealed that both GO and NaCl concentrations influence the relative extent of nanosphere formation, although the nanosphere diameter is not affected by ionic strength within our measurement ability. Nanospheres (17 nm) were observed after reducing the GO concentration by an order of magnitude (0.05 mg/mL) at identical solution ionic strength (3 mmol/L NaCl, TEM images as a function of NaCl and GO concentration are shown in Supporting Information). Likewise, decreasing the NaCl concentration by an order of magnitude (0.3 mmol/L) in 0.5 mg/mL GO revealed some 17 nm nanoclusters in a matrix of planar nanosheets.

Aqueous solutions of GO were aerosolized and rapidly dried to create super assemblies from GO nanospheres, the particle

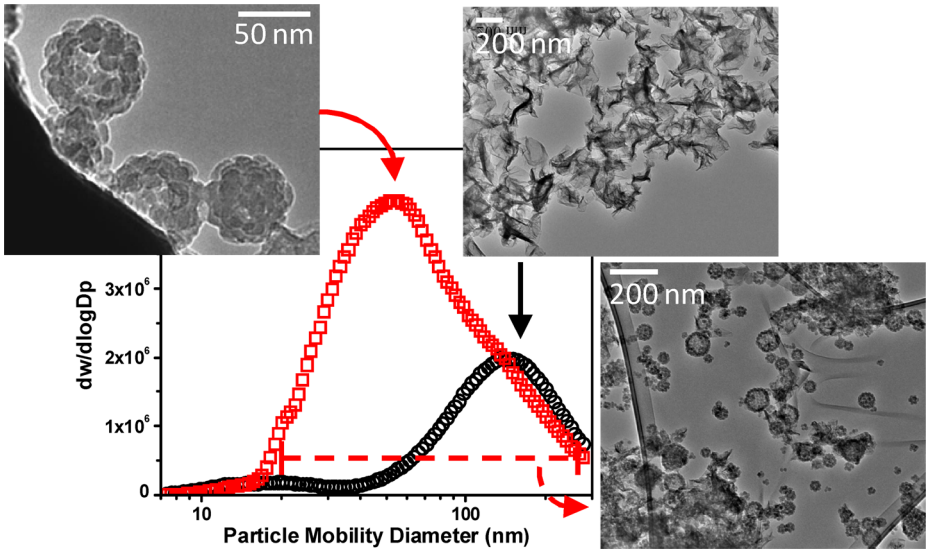

Figure 2. Dependence of ionic strength on aerosolized aqueous graphene oxide solution. Aerosol size distribution of 0.5 mg/mL GO solution from 18.2 MΩ cm H_2O (black circles) and 3 mmol/L NaCl (red squares). Insets show TEM images of crumpled GO nanosheets formed from 18.2 MΩ cm H_2O (black arrow), 70 nm super assemblies comprising 17 nm GO nanospheres from 3 mmol/L NaCl (red arrow), and full particle size distribution of GO super assemblies from 3 mmol/L NaCl (dashed red arrow).

dx.doi.org/10.1021/cm301112j | Chem. Mater. 2012, 24, 2554−2557

size distributions were measured using a scanning differential mobility analyzer (DMA) coupled to a condensation particle counter (CPC). Data for aerosolized GO solutions are shown in Figure 2. Aerosolization of GO and rapid drying from 18.2 MΩ cm H_2O forms particles that are highly crumpled and folded with a peak at ~150 nm. This peak is shifted to ~50 nm when the GO is aerosolized from a 3 mmol/L NaCl solution. TEM images reveal that the particles are super assembled clusters made from ~17 nm GO spheres, identical in size to those observed in dropcast films (additional TEM and SEM images of GO nanoclusters are shown in the Supporting Information). The full GO particle distribution from 3 mmol/L NaCl shows a few crumpled sheets (see Figure 2 inset), but the majority of the particles are GO clusters ranging from 40 nm to slightly over 100 nm. The size range of GO nanoclusters formed is dependent on the size of droplets created during the aerosolization process and on the concentration of primary GO spheres in the solution. As is the case with nanospheres, the extent of nanocluster formation is dependent on the NaCl concentration. Cluster formation was observed at NaCl concentration ≤0.5 mmol/L in 0.5 mg/mL GO, and is consistent with TEM images showing some nanosphere formation in 0.3 mmol/L NaCl concentration. TEM and particle size distributions showed that complete nanosheet to cluster conversion requires 3 mmol/L to 5 mmol/L NaCl at the GO concentrations used here.

The mass of 60 to 100 nm GO nanoclusters prepared from 3 mmol/L NaCl was measured using an aerosol particle mass analyzer.[17−21] In this size range we were assured that the aerosol stream contained minimal signal from crumpled nanosheets (mobility diameter >150 nm) or residual H_2O droplets (≤40 nm). The nanocluster mass scaled with mobility diameter and particle volume (see the Supporting Information). Using the experimentally determined cluster mass, and using cases for both random (0.36 void volume) and closed (0.24 void volume) nanosphere packing, we estimate the single GO nanosphere mass as 7.4 to 8.6 attograms (10^{-18} g). This corresponds to a nanosphere density of 2.5 ± 0.3 g/cm^3, or about 15% higher than the density of hydrated GO paper, assuming 30% H_2O content by mass.[22] Using the average nanosphere spherical volume (3.0×10^{-24} m^3) and 0.8 nm/GO sheet thickness, we calculate that GO nanospheres are comprised from 3.8×10^{-15} m^2 sheets. Using these dimensions and the GO nanosphere density, we conclude that the nanospheres of GO are solid and likely are formed from a single tightly compacted GO nanosheet (see Figure 3).

The thermal stability of GO nanoclusters was investigated by flowing aerosolized GO through a tube furnace in air (~5 s residence time at set temperature, 22% O_2) and measuring the aerosol mass *in situ*. Thermal processing of GO releases CO, CO_2, and H_2O at temperatures <220 °C to form a disordered but continuous aromatic, graphenelike framework (rGO) that is

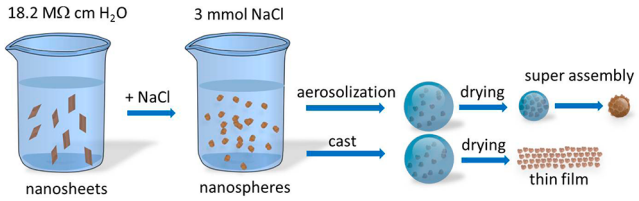

Figure 3. Experimental conditions to form nanosphere, super assemblies, and thin films from GO nanosheets.

electrically conductive.[4,16] In the presence of oxygen and at higher temperatures, GO is thermally oxidized resulting in additional mass loss. Using an aerosol particle mass analyzer (APM) we measured the aerosol mass loss as a function of thermal processing for GO nanosheets and nanoclusters. Figure 4a shows that GO nanoclusters are more thermally stable than

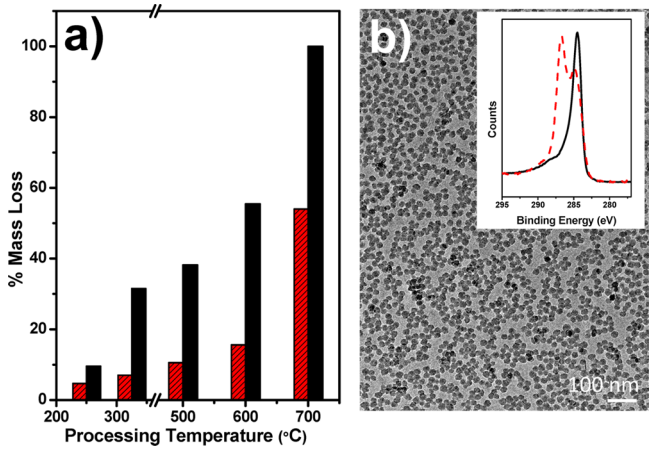

Figure 4. Effect of thermal processing of graphene oxide aerosol and thin films. (a) Percent aerosol mass loss as a function of temperature for GO nanosheets aerosolized from 18.2 MΩ cm H_2O (black) and nanoclusters from 3 mmol/L NaCl (red). (b) TEM image of submonolayer of nanospheres after thermal processing at 325 °C in air for 5 min. Inset shows XPS spectra of dropcast GO nanospheres (red) and after thermal processing (black).

nanosheets at a given thermal processing condition (temperature and residence time), even for nanosheets that are substantially larger and have higher mass. GO mass loss was nearly 50% higher for nanosheets compared to nanoclusters. Complete nanosheet mass loss via thermal oxidation was observed at 700 °C, whereas 70 nm GO nanoclusters contained slightly more than 45% of their original mass.

Thermal reduction and stability of thin films comprising GO nanospheres, similar to those shown in Figure 1b, were investigated by heating in air at 325 °C for 5 min. We previously showed using electrical conductance and X-ray photoelectron spectroscopy (XPS) that thermal processing of planar GO sheets made from the same material converted to rGO with sheet resistances of 8 kΩ sq^{-1}.[16] GO nanosphere thin films turned from light brown in color to black, consistent with film reduction. The films also retained their physical integrity. TEM images of a submonolayer film, shown in Figure 4b, revealed the nanospheres retained their conformation after thermal processing. The processing decreased the nanosphere diameter to 14.8 nm ±1.7 nm (1σ), corresponding to a loss of nearly 40% from the initial nanosphere volume. XPS data, shown in Figure 4 inset, was obtained from multilayered nanosphere films after thermal processing. Prior to thermal processing, two peaks are observed in the C 1s region, one at 284.6 eV attributed to C−C sp^2 bonds and one at 287 eV assigned to carbon bound to oxygen.[16] After thermal processing, the C 1s region consists mainly of a single C 1s component at 284.6 eV, typical of thermal reduction and formation of sp^2 rGO. Accounting for the small signal at higher binding energies associated with oxidized carbon in the XPS data, we estimate the loss of all oxygen from GO would result

dx.doi.org/10.1021/cm301112j | *Chem. Mater.* 2012, 24, 2554−2557

in a 40% mass loss from GO, consistent with the observed reduction in the nanosphere size.[1,16]

The mechanism of GO nanosphere formation may be similar to the solution ionic strength dependence observed in many biological systems.[23,24] Solution ionic strength is frequently used to change the function and structure of proteins, peptides, and cellular membranes in both the laboratory and in vivo, where ionic interactions screen charge at the nanoscale, thereby altering microscale morphology and/or function. We envision a similar mechanism occurs with GO nanosheets. We previously showed that GO made in our laboratory contains carboxylic acid and hydroxyl groups, both candidates for charge screening upon salt addition.[16] Aggregation of graphene and rGO sheets is a major challenge in their processability and utilization, and is a barrier to the scaling requirements for commercialization. The GO and rGO nanospheres both appear not to aggregate in solution and cluster only after the rapid removal of solution during aerosolization. In other words, the addition of NaCl enables intrasheet aggregation to make stable monodisperse 17 nm nanospheres that once formed do not aggregate. Aqueous nanosphere solutions are shelf stable for several months even at concentration $>1 \times 10^{16}$ nanospheres/mL. The nanosphere size is likely a result of the initial GO nanosheet areal dimensions, formed during the oxidation and exfoliation from bulk graphite. Other GO synthetic schemes and starting materials will likely vary the size of GO nanosheets, allowing for some tunability of nanosphere size. The size of GO super assemblies is highly tunable by controlling the aerosol droplet size and GO concentration. We prepared aerosols comprised of GO nanosphere dimers and trimers (24 and 30 nm mobility diameter, respectively) and were able to form super assemblies as large as 150 nm at aerosol concentrations $>1 \times 10^6$ clusters/cm^3. It is envisioned that using the tunability, stability, and simplicity to form two- and three-dimensional structures from monodisperse nanospheres demonstrated here, a new suite of multidimensional GO and rGO nanostructures is possible.

CONCLUSIONS

We demonstrated the formation of spherical, solid, monodisperse three-dimensional graphene oxide by charge screening in solution. Using this approach, GO nanospheres are able to be formed in large quantities and are shelf stable for long periods of time. Larger spherical GO super assemblies are able to be formed via aerosolization. The GO nanospheres and super assemblies are able to be thermally reduced to rGO and are more thermally stable relative to planar GO aerosol.

ASSOCIATED CONTENT

Supporting Information

Additional TEM and SEM images of GO and calculation of GO nanosphere density determination. This material is available free of charge via the Internet at http://pubs.acs.org

AUTHOR INFORMATION

Corresponding Author

*E-mail: christopher.zangmeister@nist.gov.

Author Contributions

The manuscript was written through contributions of all authors. All authors have given approval to the final version of the manuscript.

Notes

The authors declare no competing financial interest.

ACKNOWLEDGMENTS

The authors gratefully acknowledge the technical insight and aid of Drs. Donna Omiatek, Wen-An Chiou, Li-Chung Lai, The Maryland Nanocenter, and the Nanoscale Imaging Spectroscopy and Properties (NISP) Laboratory at the University of Maryland.

REFERENCES

(1) Singh, V.; Joung, D.; Zhai, L.; Das, S.; Khondaker, S. I.; Seal, S. *Prog. Mater. Sci.* **2011**, *56* (8), 1178−1271.
(2) Huang, X.; Yin, Z.; Wu, S.; Qi, X.; He, Q.; Zhang, Q.; Yan, Q.; Boey, F.; Zhang, H. *Small* **2011**, *7* (14), 1876−1902.
(3) Compton, O. C.; Nguyen, S. T. *Small* **2010**, *6* (6), 711−723.
(4) Eda, G.; Fanchini, G.; Chhowalla, M. *Nat. Nanotechnol.* **2008**, *3* (5), 270−274.
(5) Park, S.; Ruoff, R. S. *Nat. Nanotechnol.* **2009**, *4* (4), 217−224.
(6) Dreyer, D. R.; Park, S.; Bielawski, C. W.; Ruoff, R. S. *Chem. Soc. Rev.* **2010**, *39* (1), 228−240.
(7) Stankovich, S.; Dikin, D. A.; Piner, R. D.; Kohlhaas, K. A.; Kleinhammes, A.; Jia, Y.; Wu, Y.; Nguyen, S. T.; Ruoff, R. S. *Carbon* **2007**, *45* (7), 1558−1565.
(8) Becerril, H. A.; Mao, J.; Liu, Z.; Stoltenberg, R. M.; Bao, Z.; Chen, Y. *ACS Nano* **2008**, *2* (3), 463−470.
(9) Eda, G.; Chhowalla, M. *Adv. Mater.* **2010**, *22* (22), 2392−2415.
(10) Wu, J. B.; Agrawal, M.; Becerril, H. A.; Bao, Z. N.; Liu, Z. F.; Chen, Y. S.; Peumans, P. *ACS Nano* **2010**, *4* (1), 43−48.
(11) Stoller, M. D.; Park, S. J.; Zhu, Y. W.; An, J. H.; Ruoff, R. S. *Nano Lett.* **2008**, *8* (10), 3498−3502.
(12) Wang, X.; Zhi, L. J.; Mullen, K. *Nano Lett.* **2008**, *8* (1), 323−327.
(13) Ruoff, R. *Nature* **2012**, *483* (7389), S42−S42.
(14) Eswaraiah, V.; Sankaranarayanan, V.; Ramaprabhu, S. *ACS Appl. Mater. Interfaces* **2011**, *3* (11), 4221−4227.
(15) Ma, X. F.; Zachariah, M. R.; Zangmeister, C. D. *Nano Lett.* **2012**, *12* (1), 486−489.
(16) Zangmeister, C. D. *Chem. Mater.* **2010**, *22* (19), 5625−5629.
(17) Ma, X. F.; Zachariah, M. R. *J. Phys. Chem. C* **2009**, *113* (33), 14644−14650.
(18) Ma, X.; Zachariah, M. R. *Int. J. Hydrogen Energy* **2010**, *35* (6), 2268.
(19) Zhou, L.; Rai, A.; Piekiel, N.; Ma, X. F.; Zachariah, M. R. *J. Phys. Chem. C* **2008**, *112* (42), 16209−16218.
(20) Lall, A. A.; Ma, X.; Guha, S.; Mulholland, G. W.; Zachariah, M. R. *Aerosol Sci. Technol.* **2009**, *43* (11), 1075−1083.
(21) Ma, X.; Lall, A. A.; Mulholland, G. W.; Zachariah, M. R. *J. Phys. Chem. C* **2011**, *115* (34), 16941−16946.
(22) Dikin, D. A.; Stankovich, S.; Zimney, E. J.; Piner, R. D.; Dommett, G. H. B.; Evmenenko, G.; Nguyen, S. T.; Ruoff, R. S. *Nature* **2007**, *448* (7152), 457−460.
(23) Beauchamp, D. L.; Khajehpour, M. *Biophys. Chem.* **2012**, *161*, 29−38.
(24) Chen, H.; Meisburger, S. P.; Pabit, S. A.; Sutton, J. L.; Webb, W. W.; Pollack, L. *Proc. Nat. Acad. Sci. U.S.A.* **2012**, *109* (3), 799−804.